Shedding Light on Stakeholders' Perspectives for Sorbent-based Carbon Capture

Charithea Charalambous,[†,#] Elias Moubarak,[‡,#] Johannes Schilling,[¶,#] Eva Sanchez Fernandez,[§] Jin-Yu Wang,[†] Laura Herraiz,[†] Fergus McIlwaine,[†] Shing Bo Peh,[†] Matthew Garvin,[†] Kevin Maik Jablonka,[‡] Seyed Mohamad Moosavi,[‡] Joren Van Herck,[‡] Aysu Yurdusen Ozturk,[‖] Alireza Pourghaderi,[⊥] Ah-Young Song,[⊥] Georges Mouchaham,[‖] Christian Serre,[‖] Jeffrey A. Reimer,[⊥] André Bardow,[¶] Berend Smit,[*,‡] and Susana Garcia[*,†]

†*The Research Centre for Carbon Solutions (RCCS), School of Engineering and Physical Sciences, Heriot-Watt University, EH14 4AS Edinburgh, United Kingdom*

‡*Laboratory of Molecular Simulation (LSMO), Institut des Sciences et Ingénierie Chimiques, École Polytechnique Fédérale de Lausanne (EPFL), Rue de l'Industrie 17, CH-1951 Sion, Valais, Switzerland*

¶*Laboratory of Energy and Process Systems Engineering (EPSE), ETH Zurich, 8092 Zurich, Switzerland*

§*Solverlo Ltd, EH42 1TL Dunbar, United Kingdom*

‖*Institut des Matériaux Poreux de Paris, ENS, ESPCI Paris, CNRS, PSL university, Paris, France*

⊥ *Materials Science Division, Lawrence Berkeley National Laboratory, Berkeley, California 94720, United States; Department of Chemical and Biomolecular Engineering, University of California, Berkeley, California 94720, United States*

#*Contributed equally to this work.*

E-mail: berend.smit@epfl.ch; s.garcia@hw.ac.uk

Abstract

Reducing CO_2 emissions requires urgently deploying large-scale carbon capture technologies, amongst other strategies. The quest for optimum technologies is a multi-objective problem involving various stakeholders. Today's research follows a sequential approach, with chemists focusing first on material design and engineers subsequently seeking the optimal process. Eventually, this combination of materials and processes should operate at a scale that significantly impacts the economy and the environment. Understanding these impacts requires assessing factors such as greenhouse gas emissions over the lifetime of the capture plant, which usually constitutes one of the final steps. In this work, we present the PrISMa (**Pr**ocess-**I**nformed design of tailor-made **S**orbent **Ma**terials) platform, which seamlessly connects materials, process design, techno-economics, and life-cycle assessment. We compare over sixty Case Studies in which CO_2 is captured from different sources in five world regions with different technologies. These studies demonstrate how the platform simultaneously informs various stakeholders: identifying the most cost-effective technology and optimal process configuration, revealing the molecular characteristics of top-performing sorbents, determining the best locations, and informing on environmental impacts, co-benefits, and trade-offs. Our platform brings together all stakeholders at an early stage of research, which is essential to accelerate innovations at a time when they are most needed.

Introduction

We must prepare for a net-zero greenhouse gas emissions world where we cannot allow anthropogenic CO_2 to escape into the atmosphere.[1] In this world, we need to connect all kinds of sources of CO_2 (e.g., industries or waste incineration) with CO_2 sinks (e.g., geological storage or chemical industry). We must identify the optimal technology to capture the CO_2 at the source's conditions and deliver the CO_2 at the targeted sink's specifications. Importantly, the slow implementation of carbon capture in the last decades[2] has taught us that the optimal capture technology for each sink and source depends on the specific social,

economic, and regional context. Thus, the CO_2 capture challenge cannot be expected to be solved by a "one-solution-fits-all" approach.

As an alternative, this work explores tailor-made capture technologies. Solid adsorbent-based carbon capture has the potential to take advantage of modern, reticular chemistry to synthesize millions of possible adsorbents.[3] Indeed, chemists have synthesized about 100,000 novel metal-organic frameworks (MOFs) by combining organic linkers with metal nodes.[4,5] Yet, to fully explore the potential of this technology, we need to go beyond the conventional sequential, time-consuming trial-and-error approach. Computational groups explored material genomics as a first step to speed up the discovery process.[6–9] Materials are generated in silico, and molecular simulations predict their adsorption properties.[6] While these predictions are sound, the impact has been limited. The main reason is that these studies assume that the performance of a material in a capture process can be evaluated with a single or a few basic material adsorption properties (e.g., Henry selectivity or CO_2 capacity). In practice, the optimal material choice depends on the specifics of the process, scale-up, location attributes, and Life Cycle Assessment (LCA).[10–18] Due to a lack of such a system-level contextualization, materials discovery has often failed to engage the views of all stakeholders involved (see Extended Data Figure 1). To evaluate the overall performance of materials, one needs a holistic approach, which links material properties to the process design and Techno-Economic Analysis (TEA). Finally, a LCA evaluates environmental impacts beyond climate change and ensures that we do not emit more Specific carbon dioxide emissions (CO_2-eq.) than what we produce in building and operating the capture plant over its lifetime.[19] The entire life cycle captures here not only the operation of the capture plant but also its construction and disposal as well as the material synthesis and disposal.

The needed reconciliation of the views of the various stakeholders motivated our PrISMa (**Pr**ocess-**I**nformed design of tailor-made **S**orbent **Ma**terials) platform, where we seamlessly link quantum calculations, molecular simulations, process design, TEA, and LCA. Based on the crystal structure of a sorbent material, we evaluate its performance for a specific carbon

capture process, connecting a CO_2 source with a CO_2 sink in a region of the world, using a total of 50 Key Performance Indicators (KPIs).

The PrISMa platform for carbon capture

The PrISMa platform allows for the interrogation and high-throughput screening of materials for a given carbon capture Case Study. Such Case Study is defined by the CO_2 source, the destination of the CO_2 (sink), the capture technology, the available utilities, and the geographical region (see Extended Data Table 1a).

At the Materials layer, we use available experimental data or the material's crystal structure to predict the adsorption thermodynamics of the main components of the flue gas (i.e., CO_2, N_2, and H_2O) using molecular simulations. This thermodynamic data for over a thousand materials, together with process and equipment data, is the input for the Process layer. We compute process performance parameters at this layer, such as purity, recovery, productivity, and energy requirements. In the TEA layer, the economic and technical viability of the capture plant is assessed. Next, the LCA layer evaluates the environmental impacts of the carbon capture plant over its entire lifetime. By following this holistic approach, the platform identifies sets of top-performing materials. These structures can then be funneled to follow-up studies, where more detailed process models will be used and specific aspects (e.g., sorbents durability, manufacturing) investigated to bring up the technology to pilot and demonstration scale.

Informing stakeholders' perspectives

The modular structure of the PrISMa platform enables us to consider the perspectives of the different stakeholders (see Extended Data Figure 1). We compute a list of 50 KPIs (see Supplementary Information Table S5) for any combination of source, sink, technology, utilities, and region shown in Extended Data Table 1a. We carried out a Spearman analysis

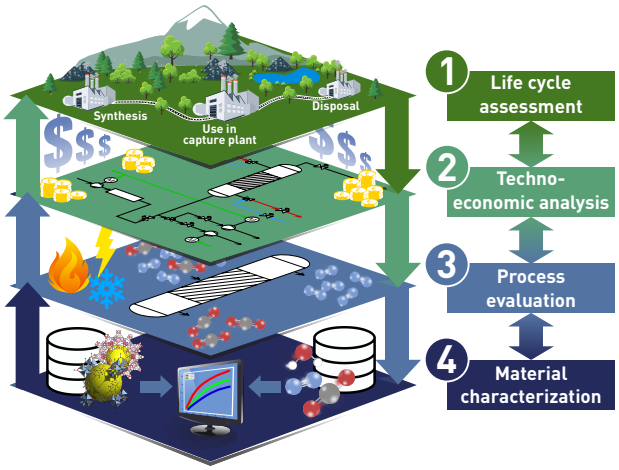

(a)

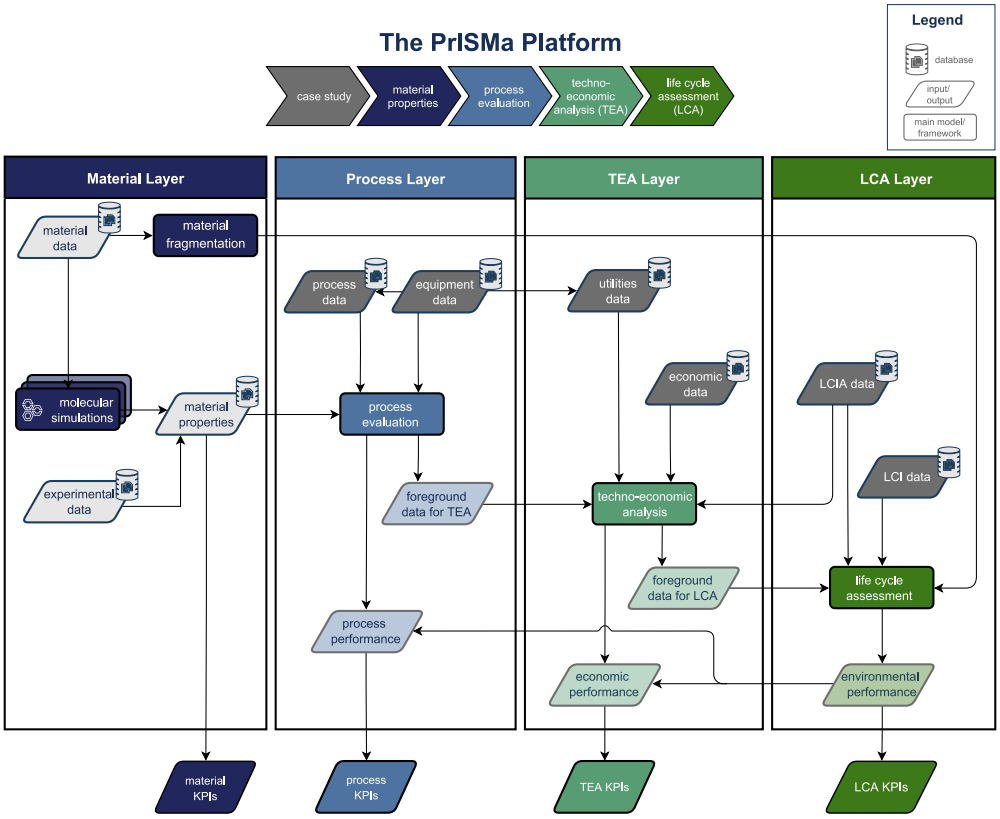

(b)

Figure 1| The PrISMa platform screens solid sorbents for CO_2 capture applications. The platform evaluates the performance of each adsorbent from material to LCA layer. (a) The four layers link life-cycle assessment (LCA), techno-economic analysis (TEA), process evaluation, and material characterization, and (b) the data flowchart in each layer. A detailed description of the methods used in each layer can be found in Supplementary Information Section 3.

of KPIs in each layer of the platform to identify a set of six reference KPIs (see Extended Data Table 1b) that encapsulate the most important trends (see Extended Data Figure 2). In the remainder, we refer mainly to these reference KPIs. Our interactive visualization tool can access all other KPIs for all Case Studies and over 1200 materials.[20]

To illustrate the use of the platform, let us first focus on one Case Study: capturing CO_2 using a Temperature Vacuum Swing Adsorption (TVSA) process (with a vacuum pressure of 0.6 bar) from a cement plant located in the United Kingdom (UK). In this study, the captured CO_2 is compressed and sent for geological storage. In Figure 2, we compare the performance of the materials for some selected KPIs with the Mono-Ethanol-Amine (MEA) benchmark[21] (see Supplementary Information Section 4); many materials outperform the benchmark for the different process, TEA, and LCA KPIs.

The Net Carbon Avoidance Cost (nCAC) is the KPI that quantifies the cost of avoiding CO_2 emissions into the atmosphere over the life cycle of the plant, and it is deemed to be the most appropriate metric to make a first selection of the most promising materials for a given application. The nCAC is not the only criterion, and evaluating materials across all KPIs and from all stakeholders' perspectives is important. For such an evaluation, we rank all materials for the reference KPIs. Figure 3 highlights the top-performing materials for a given KPI, together with their ranking on the other KPIs across the different layers of the platform. The comparison of the material rankings in Figure 3 illustrates the complexity of selecting an optimal material for a given carbon capture application; the top 10 materials for a given KPI do not necessarily perform well for the other KPIs. The holistic PrISMa approach allows for extracting relevant information for all stakeholders, as illustrated in the following sections.

The engineer's perspective: The engineer must identify and design the best technology for a separation process. In Figure 4a, we compare the nCAC of the 20 top-performing materials for the three process configurations, and for three CO_2 sources. For all three

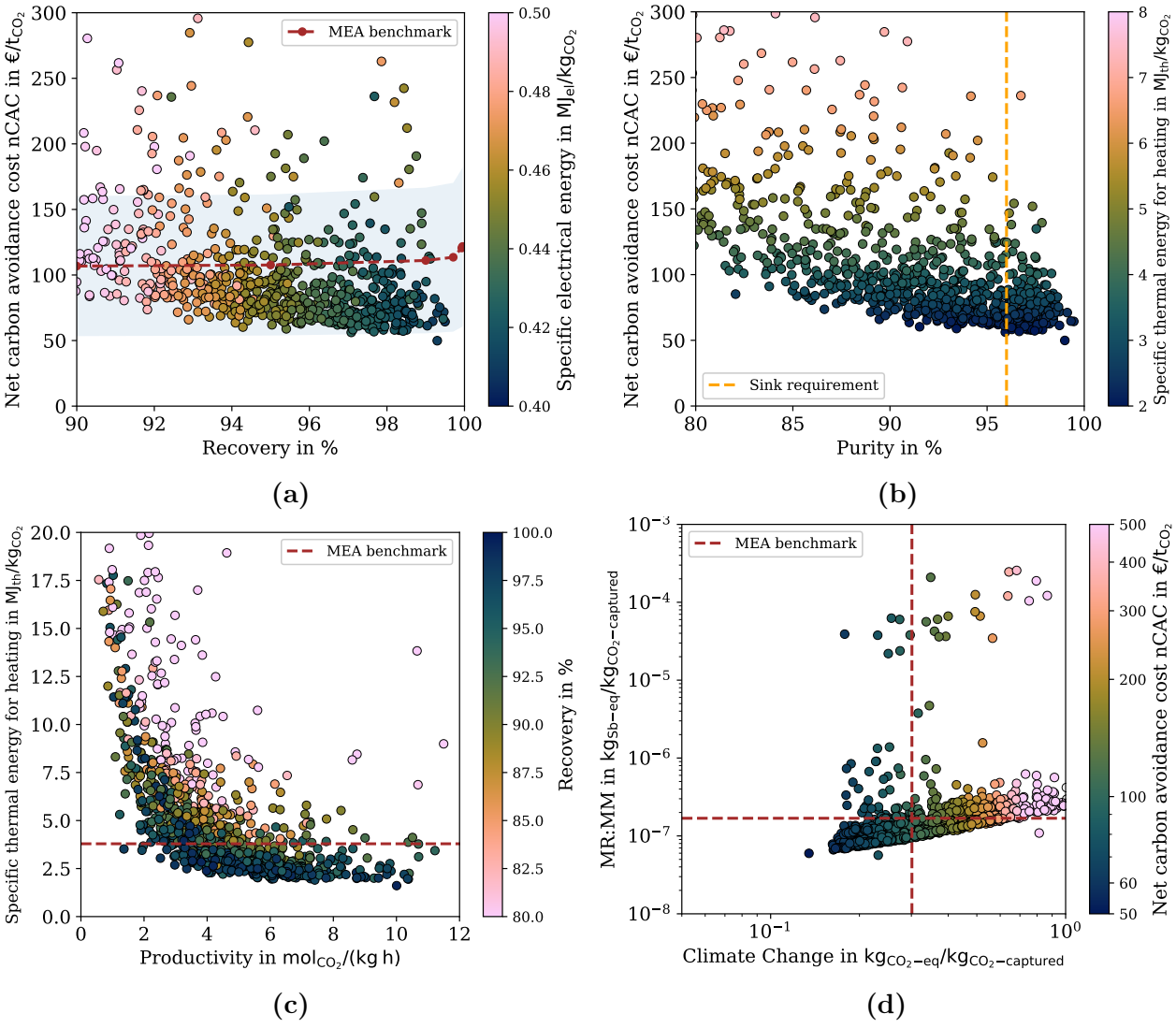

Figure 2| Materials performance for a TVSA carbon capture process at 0.6 bar **added to a cement plant in the UK.** Dotted lines in (a), (c), and (d) show the MEA benchmark (see Supplementary Information Section 4), in (b) the vertical orange dotted line gives the purity required for geological storage (>96%), and in (a) the blue shaded area gives the uncertainty. Each dot represents the corresponding KPI of a material. (a) Net Carbon Avoidance Cost (nCAC) versus recovery (R) with color coding the specific electrical energy consumption, (b) nCAC versus purity (Pu) with color coding the specific thermal energy consumption, (c) Specific thermal energy consumption for heating versus productivity (P) with color coding the recovery, and (d) Material Resources: Metals/Minerals (MR:MM) versus Climate Change (CC) with color coding the nCAC. Our visualization tool[20] gives an interactive version of this graph.

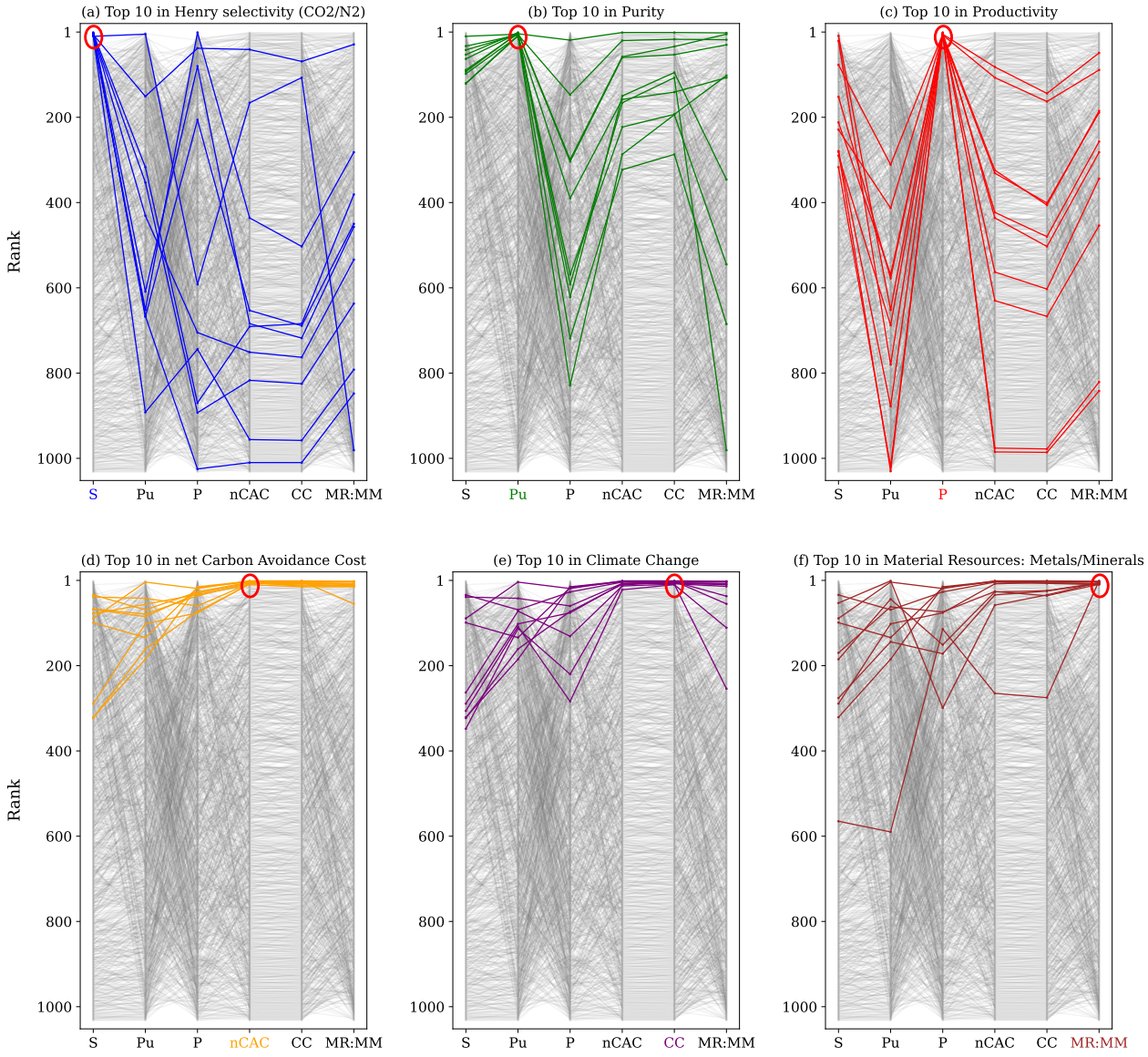

Figure 3| Comparison of materials ranking for a TVSA carbon capture process at 0.6 bar **added to a cement plant in the UK.** Rankings according to Henry selectivity (S), purity (Pu), productivity (P), Net Carbon Avoidance Cost (nCAC), Climate Change (CC), and Material Resources: Metals/Minerals (MR:MM) for a Temperature Vacuum Swing Adsorption carbon capture process added to a cement plant in the UK. In these graphs, the top-performing material is ranked number one. Colored lines represent the top 10 performers for the six reference KPIs. The same color is used to highlight the KPI of interest. Every line illustrates how the ranking of a specific material (y-axis) changes across all other KPIs (x-axis). Our visualization tool[20] gives an interactive version of this graph.

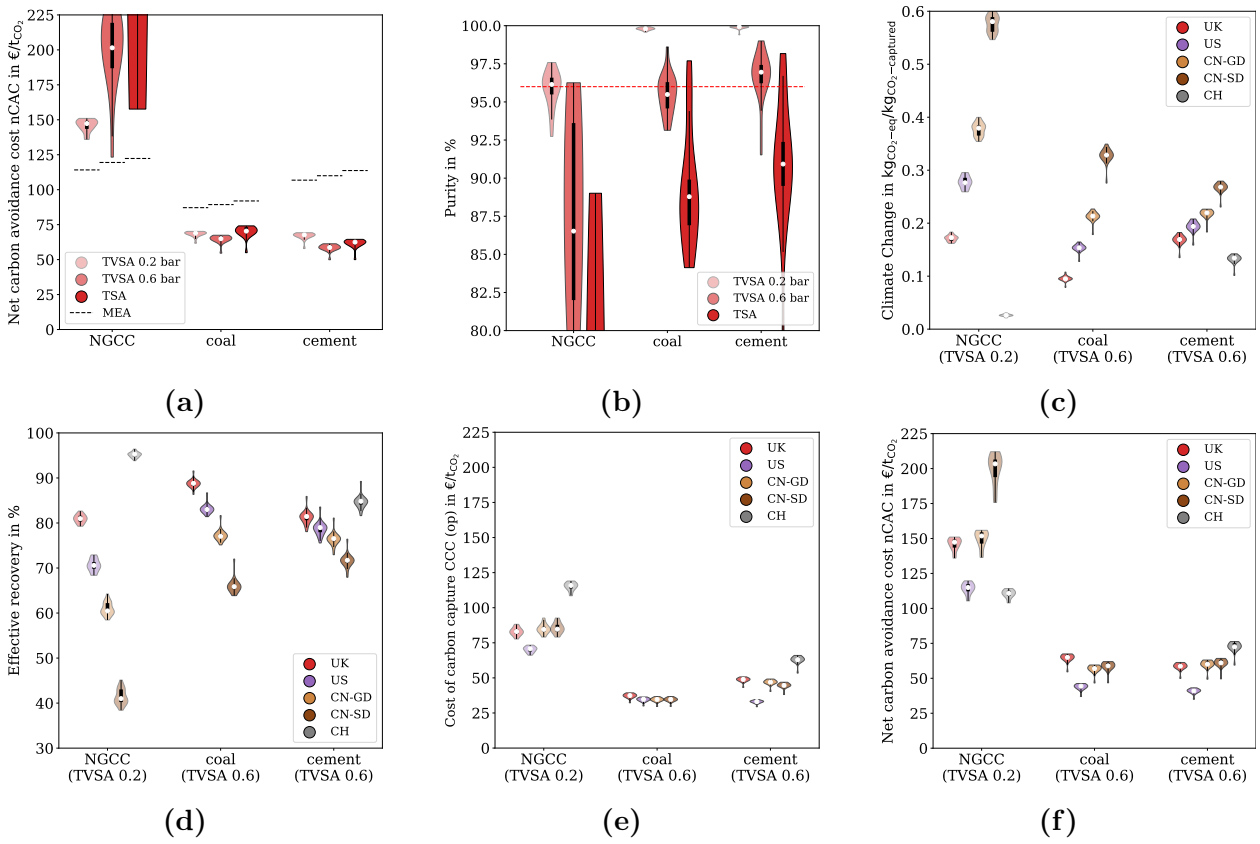

Figure 4| Comparison of process configurations and regions. This analysis of the stakeholders' perspectives focuses on the 20 materials with the lowest Net Carbon Avoidance Cost (nCAC). In these violin plots, the white circle gives the median, which we use as a (conservative) estimate of the performance. The bottom of the violin represents a few materials with an even better performance. The width indicates the number of structures with a particular y-value, and the thick black bar contains 50 % of the structures. (a) the Net Carbon Avoidance Cost (nCAC) jointly with the MEA benchmark (black dashed lines) and (b) purity for three CO_2 sources depending on the technologies (temperature swing adsorption (TSA) and vacuum swing adsorption (TVSA) with two vacuum levels 0.2 bar and 0.6 bar) jointly with the required purity of the CO_2 sink (red dashed line), the five regions' (c) Climate Change (CC) and (d) effective recovery, respectively. (e) Carbon Capture Cost (CCC) and (f) the Net Carbon Avoidance Cost (nCAC) for the five regions. See Supplementary Information Section 8 for the data.

technologies, we find materials that outperform the benchmark for coal and cement. For cases with a low CO_2 concentration in the feed stream (e.g., Natural Gas Combined Cycle (NGCC) power plants), the vacuum step in the process configuration reduces the cost, but no materials are identified with a lower nCAC than the MEA benchmark.

The vacuum step increases the purity of the product stream. This increase is achieved by rapidly purging the weakly-adsorbed components from the column's gas phase after the adsorption step but at the expense of a lower recovery than a TSA process.

Figure 4b shows that with the vacuum step, most materials in the top 20 exceed the 96 % purity, while for TSA, only a few materials meet this requirement for geological storage. Therefore, we focus the remainder on operating TVSA with 0.6 bar for the cement and coal and on the TVSA with 0.2 bar for the NGCC.

Many more materials meet the purity requirement after optimization (Supplementary Note 10.3.3). Optimization lowers the nCAC by about $7 €t_{CO_2}^{-1}$ (ca. 10%) and reduces the differences between the various process configurations. Importantly, we see that the ranking of the top-performing materials is not impacted significantly, which justifies the discussion of the non-optimized results in the remainder of this work.

The environmental manager's perspective: Running a carbon capture plant inherently produces emissions of CO_2 and other greenhouse gasses due to an increased demand for energy and materials. The environmental manager aims to maximize the captured CO_2 while simultaneously minimizing these associated CO_2-eq. emissions and other possible environmental impacts.

From this perspective, we are most interested in the cumulative quantity of CO_2-eq. avoided over the plant's lifetime. To address this, the effective recovery (see Figure 4d) adjusts the process recovery for the CO_2-eq. emissions associated with building and operating the carbon capture plant as calculated within the Climate Change KPI. For some materials, we find a CC > 1 (see Extended Data Figure 3a). A capture process with these materials will

emit more CO_2-eq. over the plant's lifetime than the total amount of CO_2 that is captured. Interestingly, some of these materials rank high in other KPIs (e.g., Henry selectivity). There can be various reasons why using such materials can result in a high impact on climate change. For instance, some of them have a very low CO_2 working capacity, leading to a huge material and energy demand per mass of CO_2 captured; others, even with comparatively good working capacities and moderate heat demands, contain metals like gold or rhodium. For these materials, the environmental impact of their synthesis phase is so large that it leads to values of CC higher than one. These findings again highlight the importance of obtaining insights into all aspects of the capture process.

An important environmental KPI is the Material Resources: Metals/Minerals, which indicates the use of minerals and metals resources over the entire life-cycle of the plant. In Extended Data Figure 4, we compare the ranking of materials based on their constituent metals, focusing on some abundant metals (Mg, Zn, and Mn) and rare metals (Co, Lu, and Ag). The MR:MM ranking will be poorer if a greater amount of the corresponding MOF is required to remove a unit of CO_2 or if the total energy demand is higher. The abundant metals rank better, while the rank drops for the rare metals. All metals spread across the entire materials, process, and economic KPIs rankings, which implies that the type of metal is not the sole determining factor in a capture process. If a MOF scores poorly on MR:MM, it may inspire chemists to explore similar structures with more abundant metals.

Another important factor in the MOF synthesis is the solvent selection. The PrISMa platform identifies the greenest solvent from a list of candidates commonly employed in practice. Anticipated environmental hot spots related to solvent selection are pinpointed in Supplementary Information Section 8.2.3.

The platform provides additional KPIs related to the process's environmental impacts (see Extended Data Figure 3b). These KPIs include the impact on the ecosystem quality, human health, and the use of resources (land, water, materials, and non-renewable energy) and allow us to flag materials that impact the environment.

The CO_2 producer's perspective: A CO_2 producer aims to find the most cost-efficient capture technology to deploy in a specific plant. For example, the host plant might offer utilities that can be integrated into the capture process, and the platform can guide the decision on whether such an integration reduces costs.

For example, a cement producer can choose different utilities, but this decision depends on the impact on the plant's environmental footprint and cost. Such analysis was conducted for Switzerland, where the CO_2-eq. emissions can be reduced using electric boilers instead of natural gas-fired ones to supply the heat demand. This replacement significantly reduces the Climate Change because of the low carbon intensity of its electricity grid and results in an almost 100 % effective recovery. This improvement comes, however, at the expense of an increase in cost by about $15\,€t_{CO_2}^{-1}$ (ca. 20%) due to the high plant operating costs in Switzerland (see Supplementary Information Section 8.2).

The investor's perspective: If one needs to perform large-scale carbon capture tomorrow, the default choice is often the well-established MEA technology. However, our platform shows that solid sorbent-based capture processes can outperform the MEA benchmark. The cost reductions increase with CO_2 concentration, and for cement, the nCAC is about a factor two lower than the benchmark. These conclusions should be an important incentive to invest in further developing these technologies.

Investors are also interested in understanding the economics of deploying carbon capture plants in different parts of the globe so they can reduce the risk of their investment. The large cost differences and electricity grid characteristics will make specific regions economically more beneficial than others. Figure 4e highlight this region-dependency for the Carbon Capture Cost (CCC). For the cement case, regional electricity and natural gas costs are low in the US, which makes it favorable in CCC, while it is highest in Switzerland. The region-dependency of coal costs is rather small, whereas, for natural gas, it is more substantial.

However, the CCC does not account for the indirect emissions associated with operating the carbon capture plant and the product loss (e.g., electricity). The Net Carbon Avoidance Cost (nCAC) corrects the system-based CCC by the Climate Change (CC) (see Figure 4d). The largest impact is observed for the NGCC case. The high CO_2-eq. emissions of the electricity grid due to the many coal power plants in China, particularly in the Shandong province, lead to the highest nCAC. In contrast, Switzerland has the lowest because its grid is dominated by hydroelectricity. The low energy cost and CO_2-eq. emissions of the electricity grid mix make the US beneficial for coal and cement.

The chemist's perspective: The route from the first synthesis of a new material to its implementation into a commercial process can take many years. It is, therefore, important to provide some guidance at the very early material's design stage on how molecular characteristics impact the material's performance.

An interesting practical question is whether one can synthesize materials that work well for any CO_2 source. Extended Data Figure 5(a) compares the nCAC ranking for NGCC and coal power plants and the cement plant. We observe a very significant change in ranking if we go from the NGCC to the coal power plant. If we move from the coal to the cement plant, the changes in the rankings are smaller but still considerable. This clearly indicates the need for tailored materials for different capture applications (see Supplementary Note 8.5.1 for more details).

In our model, we focus on wet flue gasses. Extended Data Figure 5(b) shows the increase in nCAC versus operation with dry flue gasses, and Extended Data Figure 5(a) how that performance is linked to materials' properties. An increasing value of α, i.e., water penetration in the bed, substantially increases cost, with exponential trends after a certain threshold value. For cement, the increase in nCAC is at least $4.2\,€t_{CO_2}^{-1}$ (7 %), and the impact of wet operation is amplified to as much as almost $23.4\,€t_{CO_2}^{-1}$ (20 %) for NGCC. This highlights the greater need to manage moisture at lower feed CO_2 partial pressures to en-

sure a cost-competitive process. In Supplementary Note 9, we also discuss the limits of our (ideal) model. Under non-ideal mass transfer conditions, about 60–70% of the materials still remain within top performers. However, for materials with very high water affinity (e.g., zeolite 13X), moisture slippage into the dry part of the bed can undermine their capacity, which may shift their ranking quite significantly.

Screening over a thousand materials allows us to apply data-driven methods to identify the molecular characteristics of the top-performing materials. For cement, we show that by retaining the descriptor related to the pore geometry (i.e., persistence images), we can accurately predict whether a material has a lower nCAC than the MEA benchmark (see Supplementary Information Section 8.5.3). These persistence images also rank the importance of each atom in these predictions. The collection of these atoms characterizes the molecular features that define the adsorbaphore.[22] A common theme in the materials that outperform MEA is a geometrical rod of metal atoms (highlighted in Extended Data Figure 8). These features are often correlated with stacked delocalized systems (aromatic rings) with a separation of 6 Å to 11 Å (see also Figure S62).

Extending the chemical design space

The more top-performing materials we identify, the higher the chances some materials make it to the next Technological Readiness Level (TRL). The material layer uses state-of-the-art Density Functional Theory (DFT) and molecular simulations to predict the materials' properties in the PrISMa database. These predictions require significant CPU resources but are accurate and give data that can be used for all possible Case Studies. This approach, however, does not scale to millions of materials. By leveraging the outcomes from the platform, we have implemented a Machine Learning (ML) feedback loop to screen a much larger chemical design space.

We developed an ML model that uses the crystal structure to predict whether a material

yields an nCAC above or below a given threshold. We only have a relatively limited number of top-performing materials, so we perform the training in steps. We start to train our model using an nCAC threshold corresponding to the MEA benchmark and use this model to screen a larger database. The most promising materials are added to the platform (round 1, in Extended Data Figure 9a. We now have more top-performing materials, which allows us to retrain the model with a lower threshold and perform the next rounds. Extended Data Figure 9a and Figure S84 shows that in each round, we decrease the average nCAC. Extended Data Figure 9c to 9f show the evolution of the predictions of our ML model in the chemical design space for the three thresholds. Interestingly, there is not one single cluster of top-performing materials but several clusters of chemically different materials.

The disadvantage of this approach is that a new model needs to be trained for each Case Study. We can see this for the cement case. Extended Data Figure 9b shows that the top-performing materials do not reduce the nCAC similarly. This finding is consistent with the results in Extended Data Figure 5(a), which shows that the ranking of top-performing materials for NGCC differs greatly from cement.

Experimental testing

The impact of an in silico study like our high-throughput screening is limited if it cannot reflect the actual performance of the material. As an example, we uploaded the crystal structure of a new material, MIP-212, which has 1D channels constructed from an alternation of chains of Al hydroxy-carboxylates and Cu pyrazolates (see Extended Data Figure 7 (a) and (b)). Extended Data Figure 6 shows that this is a promising material, and we studied the performance in detail (see Supplementary Note 12.1). The experimental breakthrough curves (Extended Data Figure 7b) show the separation between the column's predicted wet and dry fronts. The significant lapse between the breakthrough times of CO_2 and H_2O indicates moisture penetration below 5% of the bed length, which is in good agreement

with the predictions of our process model (further details in Supplementary Note 12.1.3). In addition, we also ranked CALF-20 in Extended Data Figure 6, which gives an nCAC of 71 €$t_{CO_2}^{-1}$. CALF-20 is being commercialized, and the estimated CO_2 capture cost for the Svante process is 50 €$t_{CO_2}^{-1}$.[23] A head-to-head comparison is, however, difficult as the two processes fundamentally differ.

Concluding remarks

The complexity and the scale of the CO_2 mitigation problem make it essential to bring all stakeholders together at an early stage. This holistic approach is presented here for a total of 63 Case Studies. The PrISMa platform provides engineers with options to identify economically and/or environmentally challenging factors in the design phase of optimal capture technologies; molecular design targets for chemists; local integration benefits for CO_2 producers; and the best locations for investors; and shows how these decisions are interrelated, de-risking investment and providing a common basis for identifying the joint way forward.

Adsorption-based technologies are very competitive, with many materials outperforming the current benchmark. Sets of promising sorbents are identified for further development, as confirmed by the experimental testing of MIP-212. These studies highlight how the PrISMa platform speeds up materials discovery and focuses Research and Development (R&D) efforts towards achievable performance targets at scale.

The impact of this approach goes far beyond carbon capture. The platform's modular design allows groups to add additional modules to extend to, for example, other gas separations, H_2 or CH_4 storage, etc. Such a bridge between fundamental research and large-scale deployment will accelerate the speed at which innovations are successfully implemented.

Data availability

All the results obtained by the platform for all Case Studies presented in this work have been deposited on Zenodo (`https://doi.org/10.5281/zenodo.8042599`). On this website, one can also find the crystal structure (cif files) of all materials studied in this work, together with the simulated isotherms, values of the heat capacity, and data that characterize the materials.

The results of this work can also be accessed through our visualization tool on the Materials Cloud `https://prisma.matcloud.xyz/`. This tool allows users to inspect all Case Studies and all KPIs. In addition, the Materials Cloud provides interactive versions of the graphs presented in this work. Updates and new Case Studies will be made available through the Materials Cloud. This tool also allows uploading the crystal structure of novel materials to be analyzed across the various Case Studies.

Code availability

The code for the analysis of the persistence images and the interactive visualization tool can be found at `https://github.com/kjappelbaum/prisma-adosorbaphore` and `https://github.com/ElMouba/PrISMa_VisTool`, respectively.

Acknowledgement

We thank Miriam Pougin, Sauradeep Majumdar, Enrique García-Díez, Benedikt Winter, and Frederick de Meyer for contributing to this work. We also thank Drs. Hasan Celik, Raynald Giovine, and UC Berkeley's NMR facility in the College of Chemistry (CoC-NMR) for spectroscopic assistance. This work is part of the PrISMa Project (299659), funded through the ACT Programme (Accelerating CCS Technologies, Horizon 2020 Project 294766). Financial contributions from the Department for Business, Energy & Industrial Strategy (BEIS), to-

gether with extra funding from the NERC and EPSRC Research Councils, United Kingdom, the Research Council of Norway (RCN), the Swiss Federal Office of Energy (SFOE), and the U.S. Department of Energy are gratefully acknowledged. Additional financial support from TOTAL and Equinor is also gratefully acknowledged. We also gratefully acknowledge Solverlo Ltd's contribution to developing the TEA module. We also acknowledge funding from the USorb-DAC Project, which is supported by a grant from The Grantham Foundation for the Protection of the Environment to RMI's climate tech accelerator program, Third Derivative. C.C., J-Y.W., L.H., and S.G. are also supported by the UKRI ISCF Industrial Challenge within the UK Industrial Decarbonisation Research and Innovation Centre (IDRIC) award number EP/V027050/1. The NMR instrument used in this work is supported by the National Science Foundation under Grant No. 2018784.

Author contributions

E.M., S.M.M., K.M.J., J.V.H., and B.S. developed the materials layer, C.C., J-Y.W., F.M., S.P., and S.G. developed the process layer, E.S.F., C.C., L.H., and S.G., developed the techno-economic analysis layer, and J.S. and A.B. developed the life-cycle assessment layer. E.M. and J.V.H. developed the visualization software. The MIP-212 MOF was synthesized and characterized by G.M., C.S., A.Y.O., A.P., A-Y.S., and J.A.R., and breakthrough curves were conducted and analyzed by M.G., F.M., S.P., and S.G. All authors contributed to analyzing the data and writing the manuscript.

Competing interest

The authors declare no competing interests.

References

(1) IEA Net Zero by 2050: A Roadmap for the Global Energy Sector. https://www.iea.org/reports/net-zero-by-2050, 2021.

(2) Martin-Roberts, E.; Scott, V.; Flude, S.; Johnson, G.; Haszeldine, R. S.; Gilfillan, S. Carbon capture and storage at the end of a lost decade. *One Earth* **2021**, *4*, 1569–1584, DOI: 10.1016/j.oneear.2021.10.002.

(3) Bui, M. et al. Carbon capture and storage (CCS): the way forward. *Energ Environ Sci* **2018**, *11*, 1062–1176, DOI: 10.1039/c7ee02342a.

(4) Furukawa, H.; Cordova, K. E.; O'Keeffe, M.; Yaghi, O. M. The Chemistry and Applications of Metal-Organic Frameworks. *Science* **2013**, *341*, 974, DOI: 10.1126/Science.1230444.

(5) Moghadam, P. Z.; Li, A.; Wiggin, S. B.; Tao, A.; Maloney, A. G. P.; Wood, P. A.; Ward, S. C.; Fairen-Jimenez, D. Development of a Cambridge Structural Database Subset: A Collection of Metal–Organic Frameworks for Past, Present, and Future. *Chem. Mater.* **2017**, *29*, 2618–2625, DOI: 10.1021/acs.chemmater.7b00441.

(6) Boyd, P. G.; Lee, Y. J.; Smit, B. Computational development of the nanoporous materials genome. *Nat Rev Mater* **2017**, *2*, 17037, DOI: 10.1038/natrevmats.2017.37.

(7) Wilmer, C. E.; Leaf, M.; Lee, C. Y.; Farha, O. K.; Hauser, B. G.; Hupp, J. T.; Snurr, R. Q. Large-scale screening of hypothetical metal organic frameworks. *Nat Chem* **2012**, *4*, 83–89, DOI: 10.1038/nchem.1192.

(8) Daglar, H.; Keskin, S. Recent advances, opportunities, and challenges in high-throughput computational screening of MOFs for gas separations. *Coord. Chem. Rev.* **2020**, *422*, 213470, DOI: 10.1016/j.ccr.2020.213470.

(9) Findley, J. M.; Sholl, D. S. Computational Screening of MOFs and Zeolites for Direct Air Capture of Carbon Dioxide under Humid Conditions. *J Phys Chem C* **2021**, *125*, 24630–24639, DOI: 10.1021/acs.jpcc.1c06924.

(10) Farmahini, A. H.; Krishnamurthy, S.; Friedrich, D.; Brandani, S.; Sarkisov, L. Performance-Based Screening of Porous Materials for Carbon Capture. *Chem Rev* **2021**, *121*, 10666–10741, DOI: 10.1021/acs.chemrev.0c01266.

(11) Leperi, K. T.; Chung, Y. G.; You, F. Q.; Snurr, R. Q. Development of a General Evaluation Metric for Rapid Screening of Adsorbent Materials for PostcombustionCO_2 Capture. *Acs Sustain Chem Eng* **2019**, *7*, 11529–11539, DOI: 10.1021/acssuschemeng.9b01418.

(12) Burns, T. D.; Pai, K. N.; Subraveti, S. G.; Collins, S. P.; Krykunov, M.; Rajendran, A.; Woo, T. K. Prediction of MOF Performance in Vacuum Swing Adsorption Systems for PostcombustionCO_2 Capture Based on Integrated Molecular Simulations, Process Optimizations, and Machine Learning Models. *Environ Sci Technol* **2020**, *54*, 4536–4544, DOI: 10.1021/acs.est.9b07407.

(13) Hu, J. Y.; Gu, X. M.; Lin, L. C.; Bakshi, B. R. Toward Sustainable Metal-Organic Frameworks for Post-Combustion Carbon Capture by Life Cycle Assessment and Molecular Simulation. *Acs Sustain Chem Eng* **2021**, *9*, 12132–12141, DOI: 10.1021/acssuschemeng.1c03473.

(14) Ajenifuja, A.; Joss, L.; Jobson, M. A New Equilibrium Shortcut Temperature Swing Adsorption Model for Fast Adsorbent Screening. *Ind. Eng. Chem. Res* **2020**, *59*, 3485–3497, DOI: 10.1021/acs.iecr.9b05579.

(15) Maring, B. J.; Webley, P. A. A new simplified pressure/vacuum swing adsorption model for rapid adsorbent screening for CO_2 capture applications. *Int. J. Greenh. Gas Control* **2013**, *15*, 16–31, DOI: 10.1016/j.ijggc.2013.01.009.

(16) Danaci, D.; Bui, M.; Dowell, N. M.; Petit, C. Exploring the limits of adsorption-based CO_2 capture using MOFs with PVSA-from molecular design to process economics. *Mol. Syst. Des. Eng.* **2020**, *5*, 35, DOI: 10.1039/c9me00102f.

(17) Taddei, M.; Petit, C. Engineering metal-organic frameworks for adsorption-based gas separations: from process to atomic scale. *Mol Syst Des Eng* **2021**, *6*, 841–875, DOI: 10.1039/d1me00085c.

(18) Balogun, H. A.; Bahamon, D.; AlMenhali, S.; Vega, L. F.; Alhajaj, A. Are we missing something when evaluating adsorbents for CO capture at the system level? *Energ Environ Sci* **2021**, *14*, 6360–6380, DOI: 10.1039/d1ee01677f.

(19) Terlouw, T.; Bauer, C.; Rosa, L.; Mazzotti, M. Life cycle assessment of carbon dioxide removal technologies: a critical review. *Energ Environ Sci* **2021**, *14*, 1701–1721, DOI: 10.1039/d0ee03757e.

(20) Moubarak, E.; Van Herck, J. Prisma Visualization Tool. https://prisma.matcloud.xyz/, 2023.

(21) Anantharaman, R.; Fu, C.; Roussanaly, S.; Voldsund, M. D3.2 CEMCAP framework for comparative techno-economic analysis ofCO_2 capture from cement plants. 2017; https://tinyurl.com/ycyk7t6y.

(22) Boyd, P. G. et al. Data-driven design of metal–organic frameworks for wet flue gas CO_2 capture. *Nature* **2019**, *576*, 253–256, DOI: 10.1038/s41586-019-1798-7.

(23) Svante Inc Carbon Capture & Removal Solutions Provider, Svante, Responds to the US's New Inflation Reduction Act. 2022; https://tinyurl.com/2s3fv6zs, Accessed: 2023-06.

Extended Data Table 1| (a) Available Case Studies in the PrISMa platform and (b) Reference Key Performance Indicators (KPIs). All Case Studies have been investigated under wet and dry feed gas conditions.

(a) Available Case Studies in the PrISMa platform. Any source, sink, technology, utility, and region in the platform can be combined. Switzerland has no coal-fired power plants, so this combination of source and region is not considered. Three technologies are available: Temperature Swing Adsorption (TSA) and Temperature Vacuum Swing Adsorption (TVSA) with two vacuum levels, 0.2 and 0.6 bar. We have a total of 63 Case Studies. The complete input parameters defining these Case Studies are in Supplementary Information Table S2.

Source	Sink	Technology	Utility	Region
NGCC Coal Cement	Geological storage	TSA TVSA - 0.6 bar TVSA - 0.2 bar	Natural gas boiler Electric boiler From host plant	UK US China (Guangdong) China (Shandong) Switzerland (CH)

(b) The six reference Key Performance Indicators (KPIs). Henry selectivity (S), Purity (Pu), Productivity (P), Net Carbon Avoidance Cost (nCAC), Climate Change (CC), and Material Resources: Metals/Minerals (MR:MM). Based on Spearman analysis, we have identified six key performance indicators that describe the most important trends in each layer of the PrISMa platform (see Supplementary Information Section 7). A description of all KPIs and data generated by the platform can be found in Supplementary Information Section 6.

KPI	Description	Definition (SI)
	Materials layer	
S	Ratio of the CO_2 and N_2 Henry's coefficients.	(6.1.2)
	Process layer	
Pu	The molar fraction of CO_2 in the product stream.	(6.2.1)
P	The amount of captured CO_2 per kg adsorbent during a process cycle	(6.2.5)
	Techno-economic analysis (TEA) layer	
nCAC	Quantifies the cost of avoiding emitting CO_2 into the atmosphere over the plant's life cycle. For power generation Case Studies, the nCAC is calculated from the levelized cost of electricity and the net carbon intensity of the plant. For cement, the nCAC is calculated from the costs of carbon capture and the Climate Change (CC), as we assume that the capture plant does not affect cement production.	(6.3.4)
	life-cycle assessment (LCA) layer	
CC	Gives the total Global Warming Potential (GWP) due to greenhouse gas emissions from the capture process to the air and CO_2 uptake from the atmosphere	(6.4.1)
MR:MM	Indicates the use of non-renewable, non-fossil natural resources (i.e., minerals and metals) and considers the availability of a mineral or metal on earth and the current mining rate. The use of natural resources like minerals and metals is measured using antimony (Sb) as reference material.	(6.4.2)

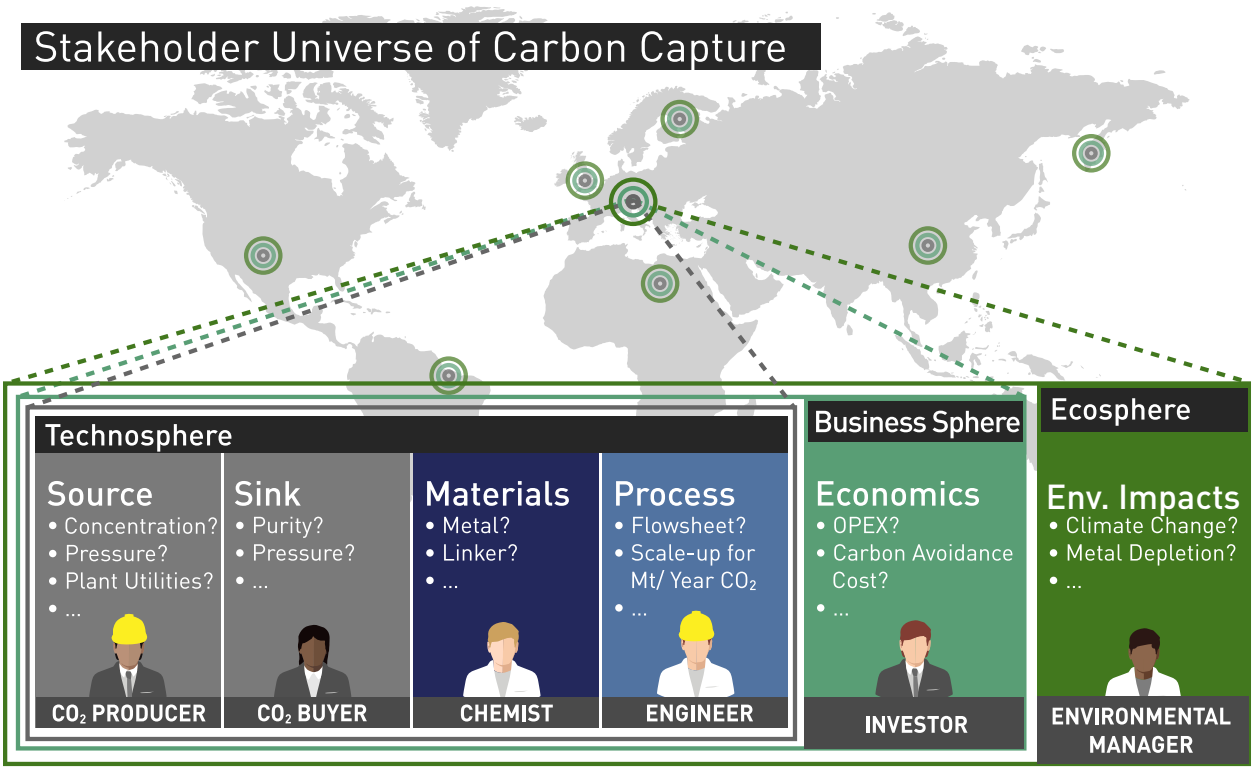

Extended Data Figure 1| Stakeholder universe of carbon capture. Illustration of the perspectives the various stakeholders have on the development of a carbon capture process.

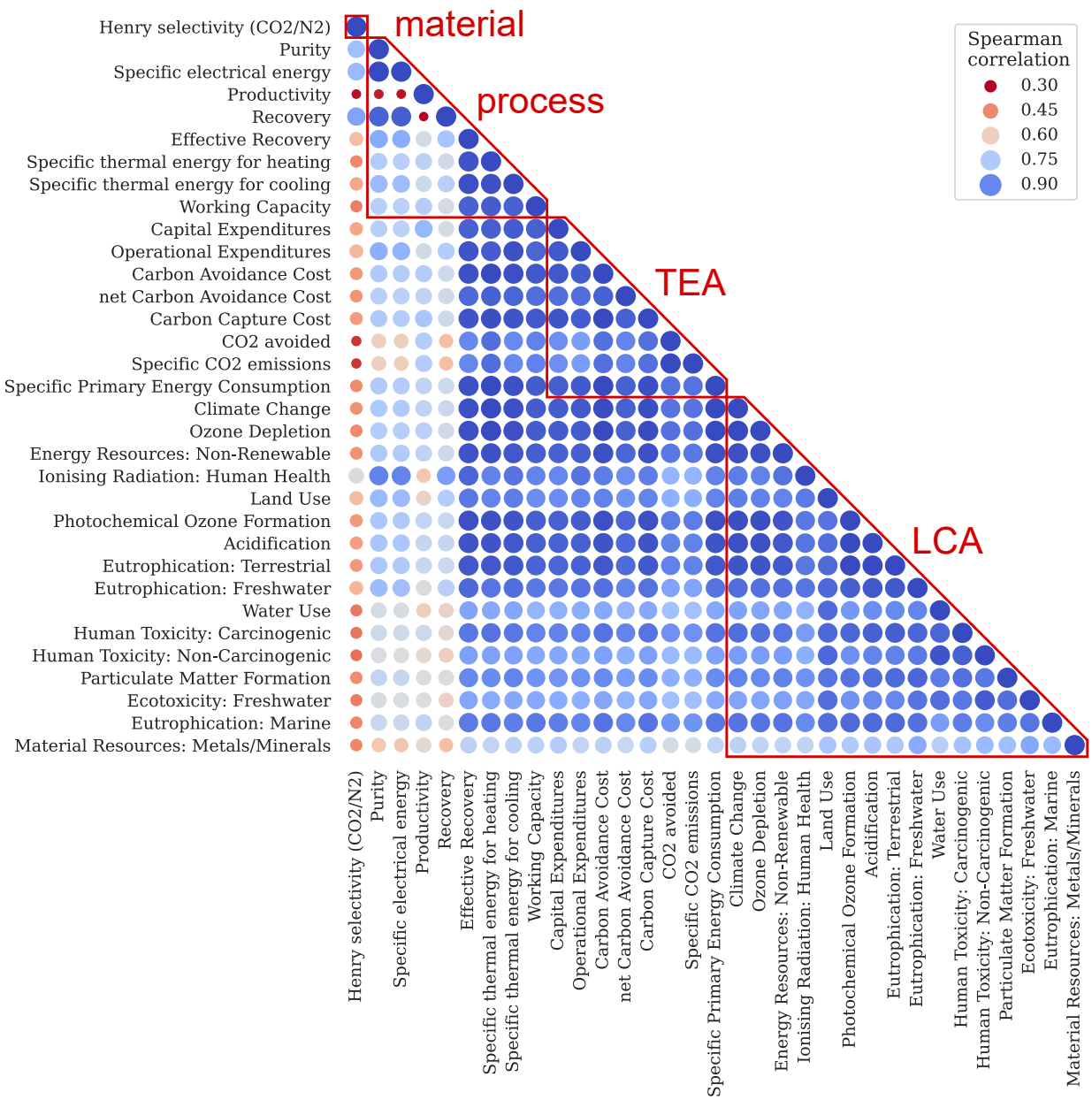

Extended Data Figure 2| Spearman's rank correlation matrix for the cement case in the UK with TVSA process at 0.6 bar**.** Spearman's rank correlation matrix of the rankings considering one material KPI, eight process KPIs, eight TEA KPIs, and 16 LCA KPIs. A dark blue color represents very strong correlations, while dark red represents lower correlations. The size of the circle is proportional to the absolute value of the correlation. The diagonal circles in the matrix have a Spearman's correlation coefficient of 1 since they represent the Spearman's correlation of a KPI with itself. A more detailed description can be found in Supplementary Information Section 7.

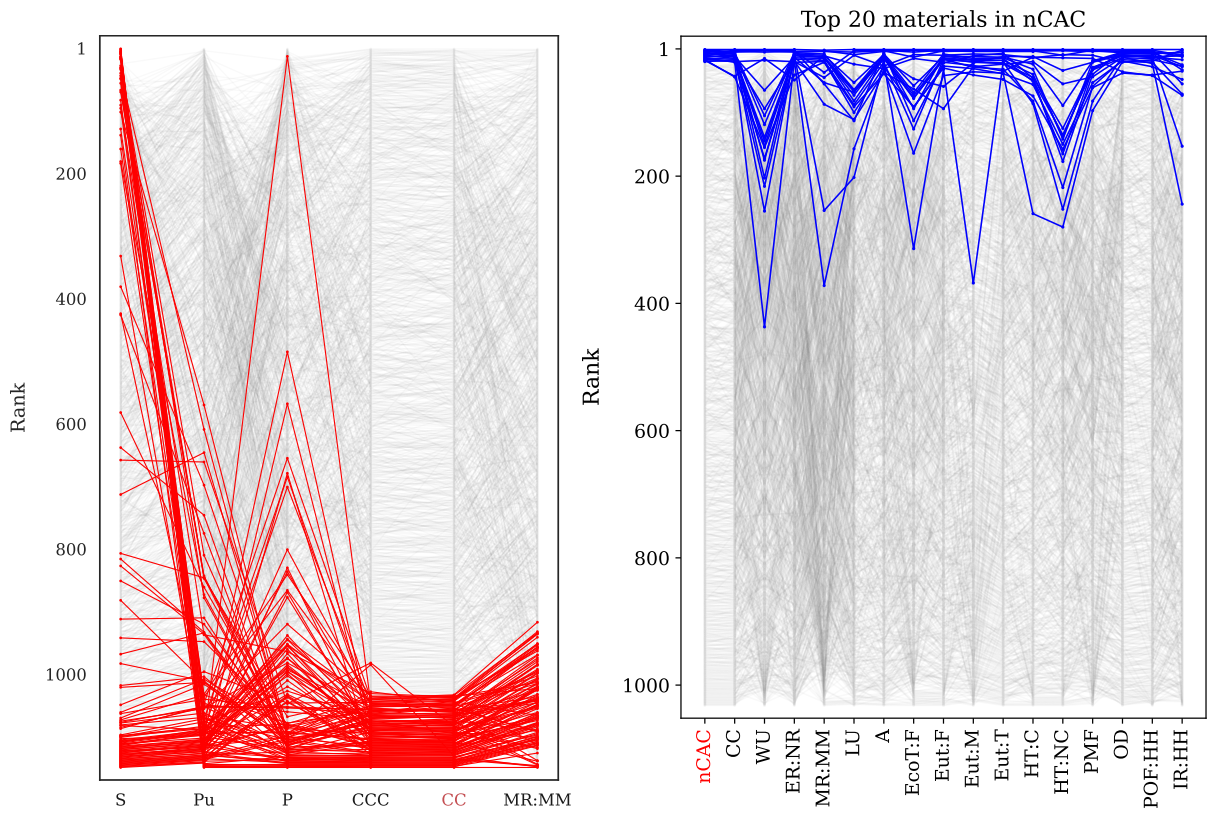

Extended Data Figure 3| Materials ranking for LCA-KPIs for cement in the UK with TVSA process at 0.6 bar**:** (a) Impact of climate change on materials ranking for materials for which more CO_2 is emitted than captured during the entire life cycle of the capture plant. The materials that are colored red have a Climate Change larger than 1, which implies that the total CO_2-eq. emissions of the capture plant using this material are larger than the amount of CO_2 that is captured. Note that we changed nCAC to the Carbon Capture Cost (CCC) (see Supplementary Information Section 6.3.6) because the nCAC is not defined for these materials. (b) Material ranking for all 16 main LCA KPIs: Climate Change (CC), Water Use (WU), Energy Resources: Non-Renewable (ER:NR), Material Resources: Metals/Minerals (MR:MM), Land Use (LU), Acidification (A), Ecotoxicity: Freshwater (EcoT:F), Eutrophication: Freshwater (Eut:F), Eutrophication: Marine (Eut:M), Eutrophication: Terrestrial (Eut:T), Human Toxicity: Carcinogenic (HT:C), Human Toxicity: Non-Carcinogenic (HT:NC), Particulate Matter Formation (PMF), Ozone Depletion (OD), Photochemical Ozone Formation: Human Health (POF:HH), and Ionising Radiation: Human Health (IR:HH). The colored lines show the top 20 materials for nCAC shown in the first column (red).

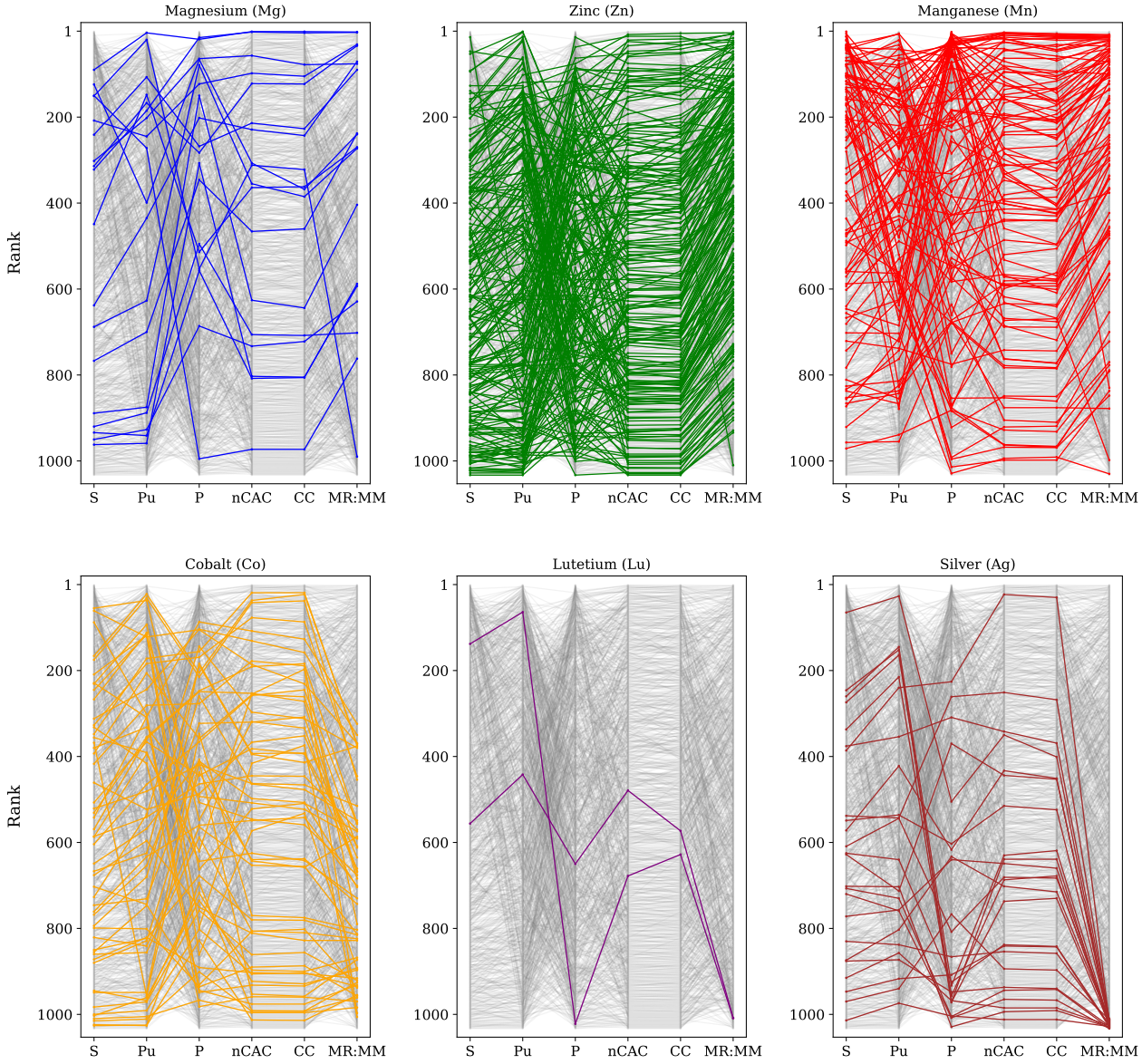

Extended Data Figure 4| Ranking of the two classes of metals for the cement case in the UK with TVSA process at 0.6 bar**.** Top: abundant metals (Mg, Zn, Mn), and Bottom: more rare metals (Co, Lu, Ag). Some MOFs contain more than one type of metal. All these metals are considered in the KPI MR:MM and can lower the ranks significantly. A combination of two or three metals is, for example, contained in the worst-performing Manganese (Mn) materials, leading to their bad performance in MR:MM compared to the other materials containing the same metal.

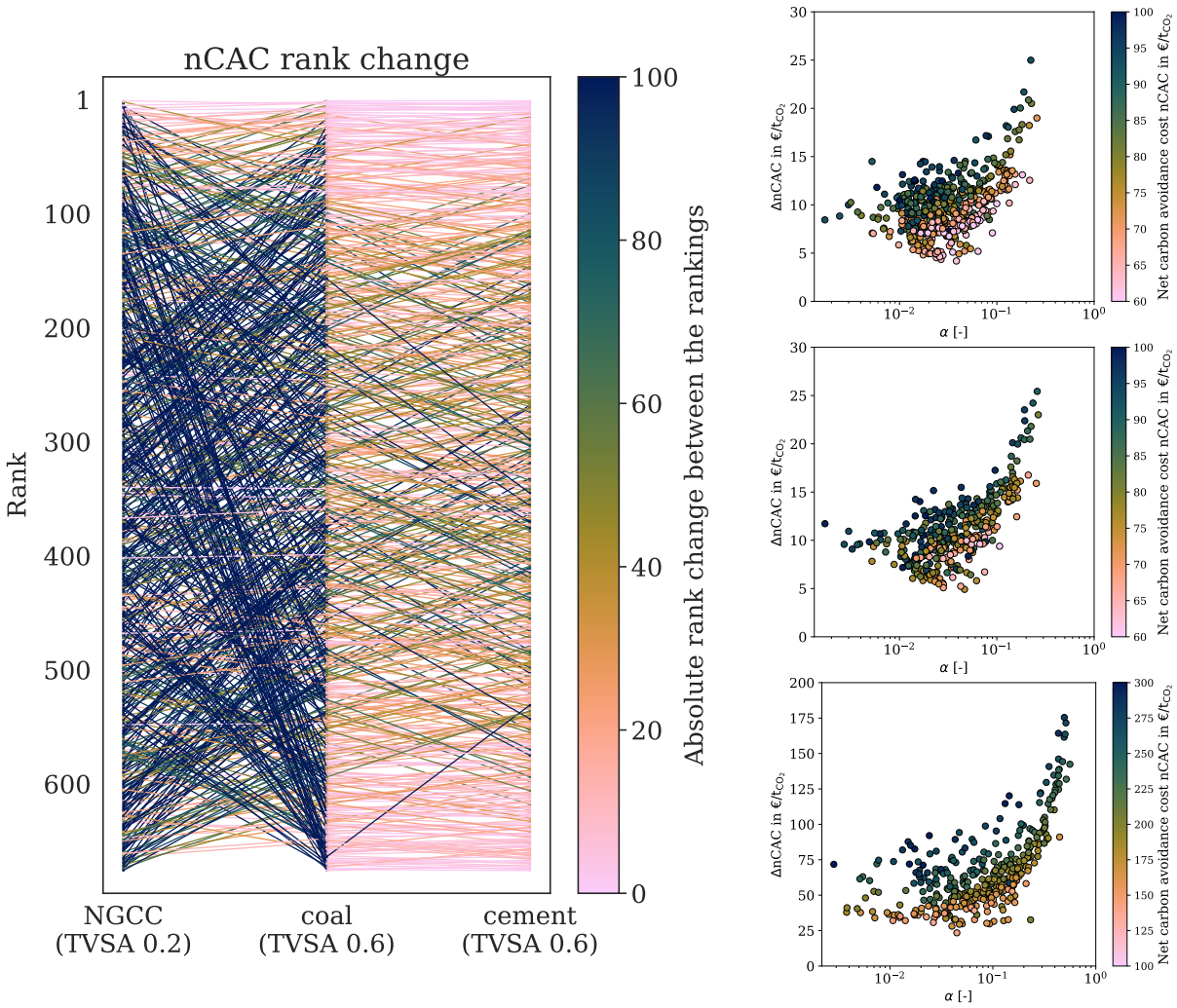

Extended Data Figure 5| Ranking of materials and comparison between wet and dry flue gasses (a) Ranking of materials for NGCC power plant (TVSA at 0.2 bar), coal power plant (TVSA at 0.6 bar), and cement plant (TVSA at 0.6 bar). The materials are ranked using the preferred technology according to the Net Carbon Avoidance Cost (nCAC). The color coding of the lines shows the number of ranks a material change ranking. (b) Scatter plots of the increase in nCAC from dry to wet conditions as a function of the fraction of bed that is moisture-loaded. (top) Cement plant (TVSA at 0.6 bar), (middle) coal power plant (TVSA at 0.6 bar), (bottom) NGCC power plant (TVSA at 0.2 bar).

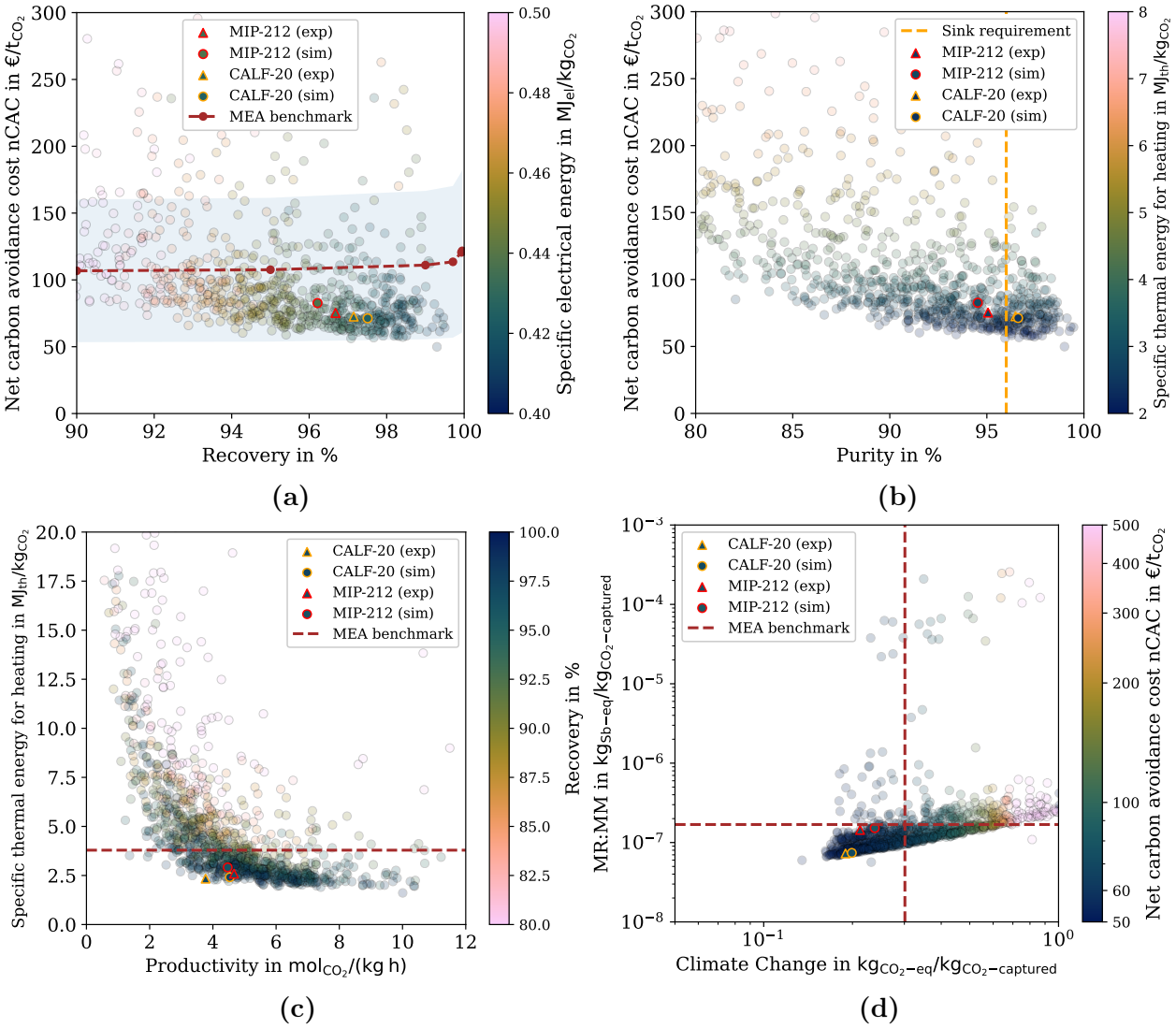

Extended Data Figure 6| Materials performance for a TVSA carbon capture process at 0.6 bar **added to a cement plant in the UK using experimental data:** The dotted lines in (a), (c), and (d) show the MEA benchmark, in (b), the vertical orange dotted line gives the purity required for geological storage ($> 96\,\%$), and in (a), the blue-shaded area gives the uncertainty. Each dot represents a material. The triangles are the structures for which experimental property data is used directly in the platform (see Supplementary Information Section 12). (a) CAC versus recovery (R) with color coding the specific energy consumption, (b) Specific energy consumption versus productivity (P) with color coding the recovery, and (c) Material Resources: Metals/Minerals (MR:MM) versus Climate Change (CC) with color coding the nCAC.

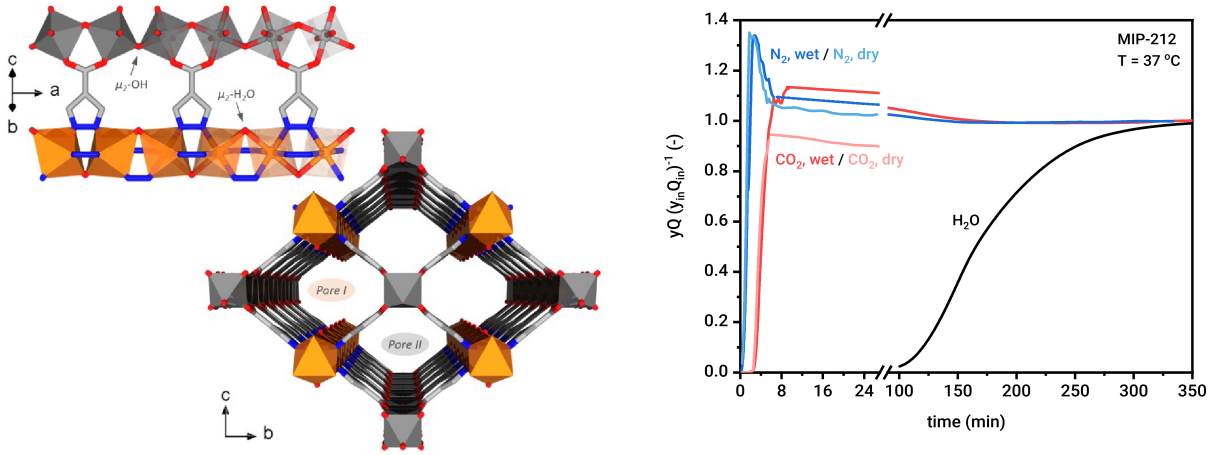

(a) **(b)**

Extended Data Figure 7| MIP-212: Panel (a) shows the structure of MIP-212. Panel (b) shows the breakthrough curve under a dry and wet flue gas and conditions corresponding to the cement Case Study.

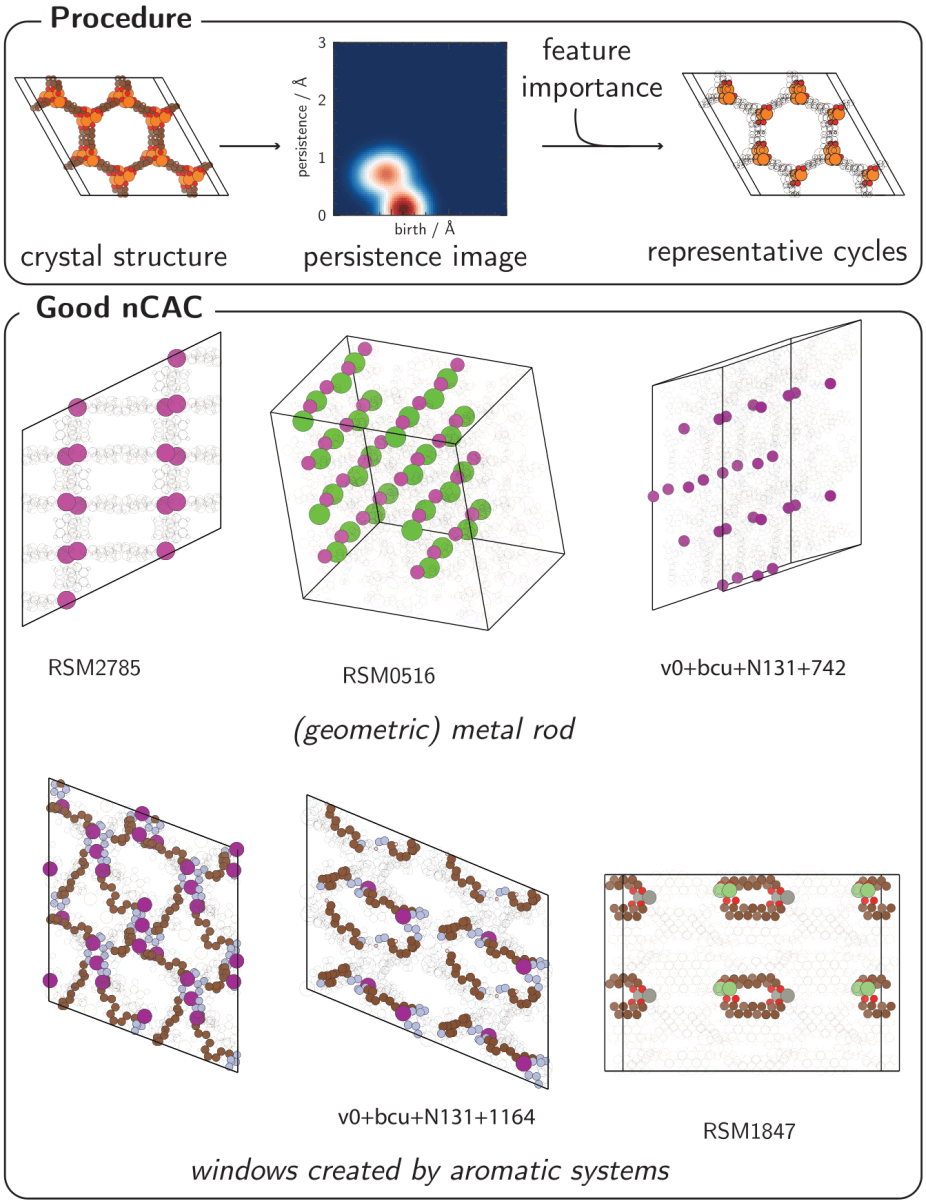

Extended Data Figure 8| Identifying the adsorbaphore for the cement Case Study (TVSA, 0.6 bar) in the UK: The top figures illustrate the methodology; the crystal structure is converted into a persistence image. We extract the most relevant pixels of the persistence images from a model trained to predict whether the nCAC is lower than the MEA-based benchmark. We then identify representative cycles, which are collections of atoms that generate a corresponding topological feature (i.e., birth/persistence pair). The bottom figure shows examples of the top-performing structures' recurring molecular features (adsorbaphores). Supplementary Information Section 8.5.3 provides more examples of these top-performing structures, and it gives the details of the methods that are used.

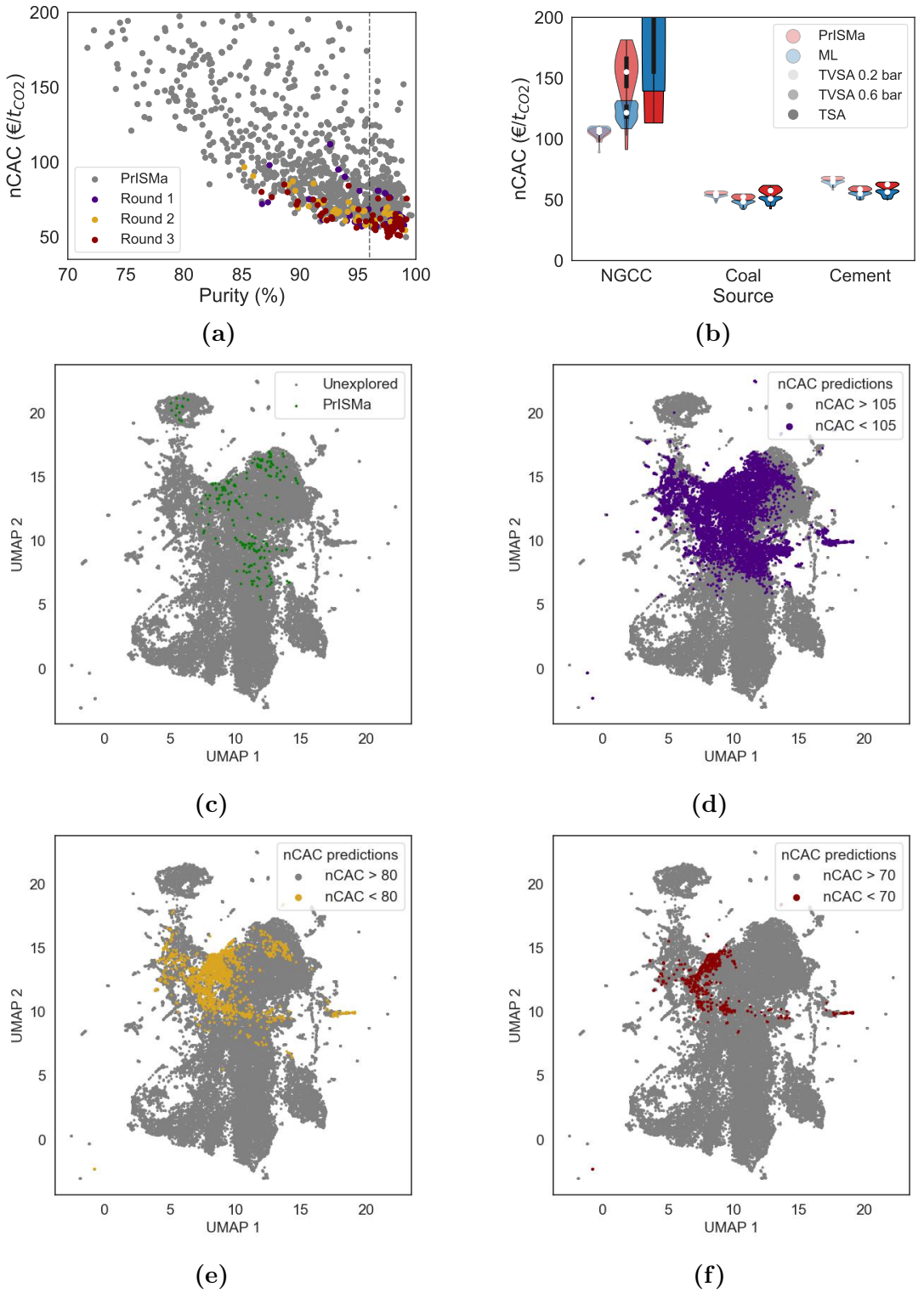

Extended Data Figure 9| Iterative material discovery: The PrISMa platform was used to train a series of ML models to predict an nCAC below a set of thresholds (105, 80, and 70 €$t_{CO_2}^{-1}$) for the cement Case Study in the UK (TVSA, 0.6 bar). (a) shows the nCAC versus purity for the different rounds. (b) shows how these materials perform for the other Case Studies. (c)–(f) visualize the screening of the chemical space through dimensionality reduction (UMAP embedding, see Supplementary Note 11). Each data point corresponds to one MOF. In (d), green dots show the ca. 1200 PrISMa MOFs, and the 30,000 grey dots are from the large database. In (c)–(f), the colored dots are MOFs with an nCAC better than the threshold.